



King's Research Portal

DOI:

[10.1073/pnas.1518934113](https://doi.org/10.1073/pnas.1518934113)

Document Version

Peer reviewed version

[Link to publication record in King's Research Portal](#)

Citation for published version (APA):

Lussignol, M., Kopp, M., Molloy, K., Vizcay-Barrena, G., Fleck, R. A., Dorner, M., Bell, K. L., Chait, B. T., Rice, C. M., & Catanese, M. T. (2016). Proteomics of HCV virions reveals an essential role for the nucleoporin Nup98 in virus morphogenesis. *Proceedings of the National Academy of Sciences of the United States of America*, 113(9), 2484-2489. <https://doi.org/10.1073/pnas.1518934113>

Citing this paper

Please note that where the full-text provided on King's Research Portal is the Author Accepted Manuscript or Post-Print version this may differ from the final Published version. If citing, it is advised that you check and use the publisher's definitive version for pagination, volume/issue, and date of publication details. And where the final published version is provided on the Research Portal, if citing you are again advised to check the publisher's website for any subsequent corrections.

General rights

Copyright and moral rights for the publications made accessible in the Research Portal are retained by the authors and/or other copyright owners and it is a condition of accessing publications that users recognize and abide by the legal requirements associated with these rights.

- Users may download and print one copy of any publication from the Research Portal for the purpose of private study or research.
- You may not further distribute the material or use it for any profit-making activity or commercial gain
- You may freely distribute the URL identifying the publication in the Research Portal

Take down policy

If you believe that this document breaches copyright please contact librarypure@kcl.ac.uk providing details, and we will remove access to the work immediately and investigate your claim.

Proteomics of HCV virions reveals an essential role for Nup98 in virus morphogenesis.

Marion Lussignol^a, Martina Kopp^{b2}, Kelly Molloy^c, Gema Vizcay^d, Roland A. Fleck^d, Marcus Dorner^{b,e}, Kierstin L. Bell^b, Brian T. Chait^c, Charles M. Rice^b and Maria Teresa Catanese^{a,b}

^aDepartment of Infectious Diseases, King's College London, London SE1 9RT, UK; ^bCenter for the Study of Hepatitis C, Laboratory of Virology and Infectious Disease, The Rockefeller University, New York, NY 10065; ^cLaboratory of Mass Spectrometry and Gaseous Ion Chemistry, The Rockefeller University, New York, NY 10065; ^dCentre for Ultrastructural Imaging (CUI), King's College London, London SE1 9RT, UK; ^eSection of Virology & Section of Hepatology, Imperial College London, London W2 1PG, UK.

Submitted to Proceedings of the National Academy of Sciences of the United States of America

Hepatitis C virus (HCV) is a unique enveloped virus that assembles as a hybrid lipo-viral particle by tightly interacting with host lipoproteins. As a result, HCV virions display a characteristic low buoyant density and a deceiving coat, with host-derived apolipoproteins masking viral epitopes. We previously described methods to produce high-titers preparations of HCV particles with tagged envelope glycoproteins that enabled ultrastructural analysis of affinity-purified virions. Here, we performed proteomics studies of HCV isolated from culture media of infected hepatoma cells to define viral and host-encoded proteins associated with mature virions. Using two different affinity purification protocols, we detected 4 viral and 46 human cellular proteins specifically co-purifying with extracellular HCV virions. We determined the C terminus of the mature capsid protein and reproducibly detected low levels of the viral nonstructural protein, NS3. Functional characterization of virion-associated host factors by RNAi identified cellular proteins with either pro- or anti-viral roles. In particular, we discovered a novel interaction between HCV capsid protein and the nucleoporin Nup98 at cytosolic lipid droplets that is important for HCV propagation. These results provide the first comprehensive view of the protein composition of HCV and new insights into the complex virus-host interactions underlying HCV infection.

enveloped virus | hepacivirus | virion proteomics | virus assembly | virus-host interactions

Introduction

Compositional studies of virions provide powerful clues for understanding the functions of viral proteins, assembly and entry pathways and more broadly, mechanisms of virus-host interactions. Increasingly sensitive mass spectrometry techniques have enabled the detection of viral and cellular proteins that are incorporated in virions even at very low levels (1).

Hepatitis C virus (HCV) is a positive-sense, single stranded RNA virus of the *Flaviviridae* family. This bloodborne pathogen causes chronic liver infection that develops into cirrhosis and hepatocellular carcinoma and is the leading indication for liver transplantation. Over 185 million people are chronically infected with HCV (2). Despite great advances in the ability to study this virus *in vitro*, significant gaps remain in our understanding of the infectious particle and the virus-host interactions required for HCV propagation.

The protein composition of HCV is not known. While the capsid protein, Core, and the E1 and E2 envelope glycoproteins are thought to be the major constituents of the virion, it remains to be determined if nonstructural (NS) viral proteins are packaged as well. A growing body of literature suggests that cellular proteins are important components of HCV. Indeed, this virus closely associates with low- (LDL) and very-low density lipoprotein (VLDL) components, forming a chimeric lipo-viral particle (LVP). Biochemical and ultrastructural studies demonstrated that infectious HCV particles are coated with endogenous apolipoproteins that play key roles in viral attachment and entry,

explaining the higher infectivity of lipoprotein-associated HCV (2).

The heterogeneous size and appearance of extracellular HCV, ranging from 40 to >100 nm in diameter, suggests that the set of associated proteins (both viral and cellular), as well as their stoichiometry, might vary across the virion population. Additionally, the specific infectivity of HCV changes according to the cell system/host that the virus is produced in, highlighting a strong contribution of the host to the makeup of the virus particles (2). Therefore, a proteomic analysis of HCV represents an attractive means of discovering novel virus-host interactions with possible implications for understanding exploitation/subversion strategies that this chronic virus uses to persist within the host.

We recently described two methods for producing and affinity purifying high titers of cell culture derived HCV (HCVcc) that enabled ultrastructural analysis of HCV virions (3). The first was based on the construction of an infectious clone with tags fused at the N-terminus of E2, while the second relied on the use of potent HCV neutralizing antibodies.

In this study, we used both affinity-purification approaches to perform proteomic analysis of extracellular HCV virions. We established that Core¹⁷⁷ (aa 1-177) is the form incorporated in mature HCV particles and detected a number of virion-associated virus and host-derived proteins. Functional characterization of HCV-associated cellular proteins identified new host factors, including a nuclear pore complex protein, that participate in HCV infection.

Significance

Virion proteomics represents a powerful and unbiased approach to gain insights into the process of virus assembly and the host factors important for infection. For hepatitis C virus (HCV), it is known that infectious virions are assembled alongside endogenous lipoproteins to give rise to a chimeric lipo-viral particle. Host-derived apolipoproteins coat the exterior of circulating particles, making for a veiled pathogen. The protein composition of HCV remains, however, undefined. Here, using mass spectrometry, we identified novel viral and cellular proteins specifically associated to HCV virions and discovered an essential interaction between the capsid protein and the nucleoporin Nup98 that is required for virion biogenesis.

Reserved for Publication Footnotes

137
138
139
140
141
142
143
144
145
146
147
148
149
150
151
152
153
154
155
156
157
158
159
160
161
162
163
164
165
166
167
168
169
170
171
172
173
174
175
176
177
178
179
180
181
182
183
184
185
186
187
188
189
190
191
192
193
194
195
196
197
198
199
200
201
202
203
204

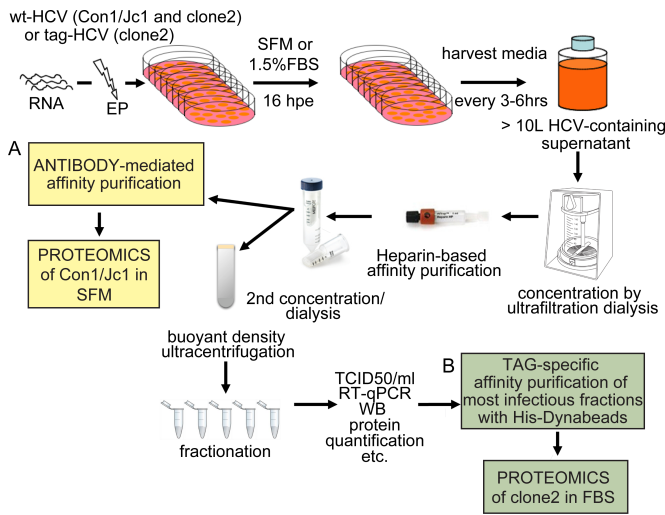


Fig. 1. HCV purification flowchart. Schematic description of the steps used to purify extracellular HCV virions.

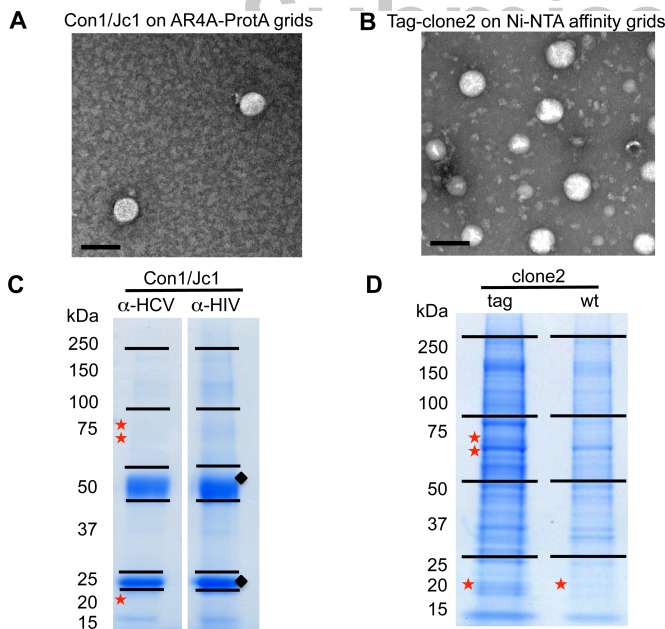


Fig. 2. Analysis of purified HCV virions. (A-B) TEM images of purified HCV particles used for proteomics studies. Scale bars, 100nm. (C-D) Coomassie staining of SDS-PAGE gels subjected to proteomics analysis. Stars indicate the slices where E2, NS3 and Core (top to bottom) were detected; diamonds show the heavy and light antibody chains. **Table 1.** Viral proteins in purified HCV virions.

Results

Purification of extracellular HCV virions. Several challenges hampered compositional studies of patient-derived virus or HCV grown in primary hepatocyte cultures. These include the presence of neutralizing antibodies in the plasma of infected patients that interfere with the isolation of circulating virions, the high background from serum proteins, the limited availability, prohibitive costs and short survival of primary human hepatocytes in cell culture, as well as their low permissiveness to HCV infection. In contrast, large volumes of HCVcc-containing supernatants can be produced in serum-free or low serum-containing media and viral envelope proteins can be tagged to facilitate virion affinity purification. Large-scale electroporations of HCV RNA into Huh-

Table 1. Viral proteins in purified HCV virions.

Protein		tag-HCV	wt-HCV	□-HCV	□-HIV
E2	Log (e)	-23	-	-18	-
	Seq cov corr	34	-	35	-
	Unique	3	-	3	-
CORE	Log (e)	-130	-9	-94	-
	Seq cov corr	85	14	36	-
	Unique	13	1	9	-
NS3	Log (e)	-3.7	-	-3.4	-
	Unique	1	-	1	-
	Sequences	SIDFIPVETLDVVTR	-	APITAYAQQTR	-

A MSTNPKPQRKTKRNTNRRPQDVKEPGGQIVGGVYLLPRGRPRLGVRATRKTSER
SQPRGRRQPIPKDRRSTGKSWGEPGPWPPLYGNEGLGWAGWLLSPRGRSRPSWG
PNDRPHRRSRNVGKVIDITLCGFADLMGYIPVVGAPLGGVARALAHGVRVLEDGVNE
ATGNLPGCSFSIFLLALLSCITTPVSA

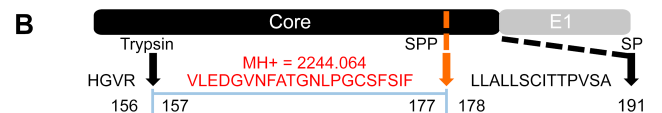


Fig. 3. Identification of the C-terminus of mature Core in extracellular HCV virions. (A) Amino acid sequence of Core corresponding to residues 1-191 of the J6 HCV polyprotein, genotype 2a. The underlined sequences were identified in the database search. Trypsin cleavage sites are shown in bold, while the most C-terminal peptide cleavage site is shown in red. (B) Schematic representation of the junction between Core and E1. The predicted sequence and calculated protonated masses (MH+) of clone 2 Core peptide generated by cleavage with exogenous Trypsin protease and the host signal peptide peptidase (SPP) are indicated in red and match the observed data. Full length Core (191 aa) is generated by cleavage of the signal peptidase (SP), while mature Core is produced by SPP-mediated cleavage at position 177. **Table 2.** HCV-associated cellular proteins selected for follow-up studies.

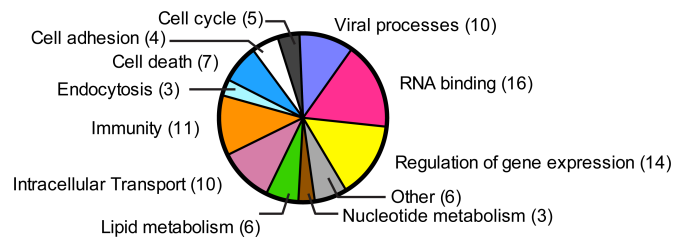


Fig. 4. Functional classification of host proteins in HCV virions according to their known cellular functions.

7.5.1 hepatoma cells were carried out and cell supernatants were harvested every 3-6 hours up to 120 hours post-electroporation and stored at 4C to minimize temperature-dependent inactivation of HCV (Fig. 1). Between 12 and 15 liters of HCV-containing media were produced and concentrated in a nitrogen-pressurized ultrafiltration cell using low protein-binding membranes with a molecular weight cut off (MWCO) of 100kDa that retained >85% of the viral infectivity (Fig. S1C and Table S1). Two sequential affinity purification steps were used to enrich for envelope-containing particles. The first one relied on a high-affinity interaction between heparin and E2. Although the heparin-eluted

Table 2.

#	Identifier	Gene name	Protein name	Log (e)	n. spectra	MW (kDa)	Gel slice
1.	ENSP00000351416	ANKRD17	Ankyrin repeat domain 17	-54.9	9	274.1	A
2.	ENSP00000448366	SCYL2	SCY1-like 2	-18.1	3	77	A
3.	ENSP00000392423	RELN	Reelin	-7.9	3	388.1	A
4.	ENSP00000376899	PTGFRN	Prostaglandin F2 receptor inhibitor	-54.3	12	98.5	B
5.	ENSP00000295598	ATP1A1	ATPase, Na ⁺ /K ⁺ transporting, alpha 1 polypeptide	-27.4	5	112.8	B
6.	ENSP00000316032	NUP98	Nucleoporin 98kDa	-17.3	6	195.7	B
7.	ENSP00000367122	SLC3A2	Solute carrier family 3, member 2	-23.8	4	68	C
8.	ENSP00000264883	NUP54	Nucleoporin 54kDa	-14.3	6	55.4	C
9.	ENSP00000387282	AGFG1	ArfGAP with FG repeats 1	-7.7	3	60.7	C
10.	ENSP00000260130	SDCBP	Syndecan binding protein (syntenin)	-10.7	3	32.4	E
11.	ENSP00000221566	SGTA	Small glutamine-rich tetratricopeptide repeat-containing, alpha	-10.3	3	34	E
12.	ENSP00000227525	TMEM109	Transmembrane protein 109	-35.2	15	26.2	G

Determination of HCV-associated cellular proteins by mass spectrometry.

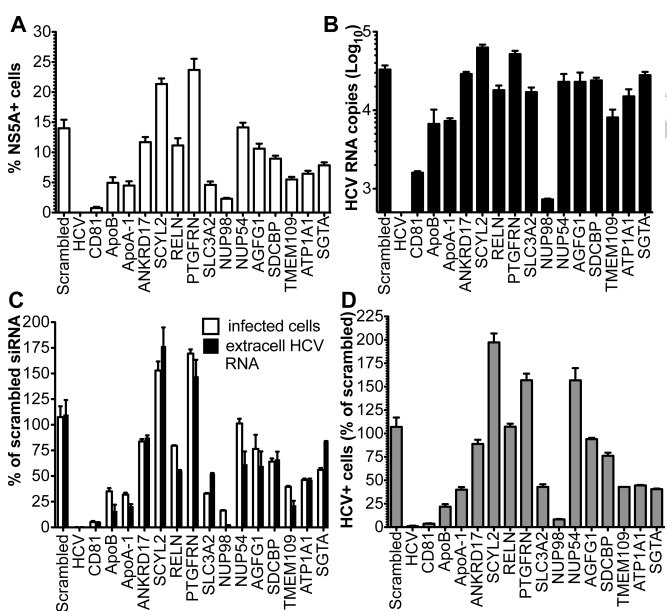


Fig. 5. Validation of cellular proteins incorporated in HCV virions by RNAi. Huh-7.5 cells were transfected with siRNA smartpools against the indicated molecules and infected 48 hours later with Con1/Jc1 at low MOI (0.05). (A, C) The percentage of HCV⁺ cells was determined 3 dpi by NS5A staining and FACS analysis (white bars). (B, C) The number of HCV RNA genomes released in the cell media was quantified by RT-qPCR (black bars). (D) The infectivity of HCV particles produced by siRNA-transfected cells was assessed by inoculating equal volumes of cell culture media on naïve Huh-7 cells. The number of NS5A⁺ cells was determined by FACS 3 dpi. In C-D, data are expressed as percentage of scrambled siRNA.

material contained less than 50% of the input viral genomes, a striking increase in the specific infectivity (FFU/genome RNAs) of the particles was noted (from approximately 1/4000 for the input material to 1/5 post-heparin purification; Table S1 and Fig. S1B-C). This suggests that the heparin purification step eliminates non-infectious RNA-containing particles and may additionally remove factors inhibiting HCV infectivity. The heparin column also removed >95% of the protein contaminants present in the concentrated culture supernatant (Fig. S1A). The second affinity purification step consisted of either antibody- or tag-mediated capture of envelope containing HCV particles. In the first case, a Con1-Jc1 virus with five adaptive mutations was produced in serum-free media (SFM), concentrated, heparin-

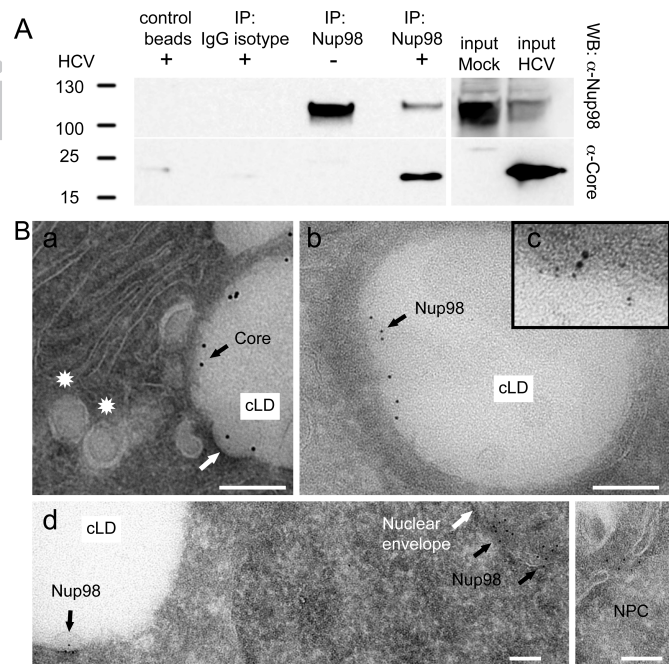


Fig. 6. Nup98 interacts with Core and re-localizes to cLDs in infected cells. (A) Cell lysates from naïve and clone2-infected Huh-7.5 cells (6 dpi) were immunoprecipitated with anti-Nup98 antibody. Beads without antibody (control beads) or conjugated to isotype-matched IgG served as negative controls. Immunoblot analysis with anti-Nup98 and anti-Core antibodies are shown. (B) Huh-7.5 cells infected with clone2 for 4 days were cryo-sectioned and stained with antibodies to (a) Core, (b, d) Nup98 or (c) both. Representative iEM images are shown. (a) Core is enriched on cLDs juxtaposed to ER membranes. Membrane curvature may represent a nucleocapsid budding event (arrowhead). Spherical particles within vacuoles may be HCV virions at early maturation stage (stars). (c) Co-staining with Core (12nm) and Nup98 (6nm)-specific antibodies. (d) A low magnification image shows the expected localization of Nup98 on both sides of the nuclear envelope, in the central channel of the nuclear pore complex (NPC, see insert), and the additional presence of Nup98 on cLD. Scale bars, 100 nm.

purified and incubated with a potent HCV-neutralizing antibody that recognizes a discontinuous epitope encompassing E1 and E2 (AR4A; (4); Fig. 1A). For tag-mediated affinity purification, we used a J6/JFH1 clone 2 infectious genome with a six histidine (6xHis) tag and two copies of a Strep tag II fused to the N-terminus of E2 (tag-clone 2; (3)) that was harvested in 1.5%

409
410
411
412
413
414
415
416
417
418
419
420
421
422
423
424
425
426
427
428
429
430
431
432
433
434
435
436
437
438
439
440
441
442
443
444
445
446
447
448
449
450
451
452
453
454
455
456
457
458
459
460
461
462
463
464
465
466
467
468
469
470
471
472
473
474
475
476

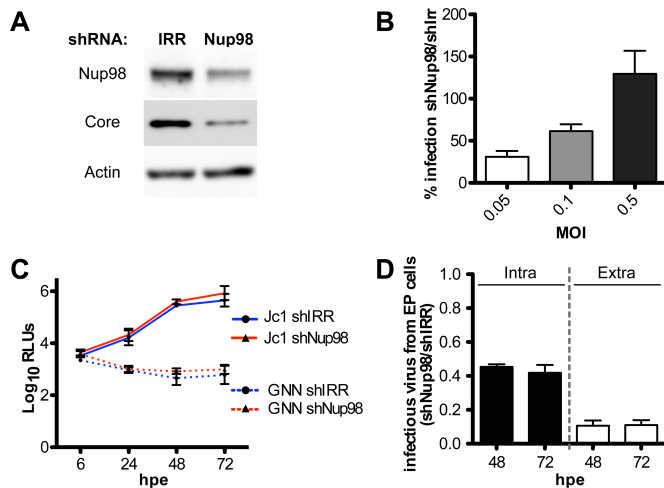


Fig. 7. Impact of Nup98 on the HCV life cycle. (A) Immunoblot analysis showing Nup98 and Core expression in Huh-7.5 expressing either shIRR or shNup98 3 days post infection with HCV clone2. (B) shIRR or shNup98 cells were infected with clone2 at the indicated MOI for 3 days and the % of NS5A⁺ cells was determined by FACS analysis. Data are expressed as % of infection measured in shNup98 compared to shIRR. (C-D) ShIRR and shNup98 cells were electroporated with Jc1FLAG2(p7-nsGluc2A) and Jc1FLAG2(p7-nsGluc2A)/GNN RNAs. (C) Kinetics of luciferase secretion in cell culture media was measured between 6 and 72 hours post electroporation (hpe) to monitor viral RNA translation and replication. AR4A was added to the culture media at 1µg/mL to minimize secondary rounds of infection. (D) Intracellular and extracellular virus harvested from shNup98 and shIRR cells at 48 and 72 hpe were inoculated onto naïve Huh-7.5. Infectivity was assessed by luciferase quantification and is shown as ratio of infection obtained with inocula derived from shNup98 compared to shIRR cells

FBS (Fig. 1B). Tandem affinity purification using His-Dynabeads and Streptactin beads was attempted but proved unsuccessful. This might be partly due to particle aggregation post-elution (Fig. S1F). His-Dynabeads resulted in lower background than MagStrep beads and were therefore used for tag-mediated virion purification (3). Production of HCV in FBS-containing media yielded higher titer stocks than SFM. Moreover, tag-specific purification methods capture more virions compared to antibodies targeting HCV glycoproteins (Fig. 2A; (3)). As a result, tag-HCV but not Con1-Jc1 was subjected to buoyant density fractionation prior to the second affinity capture step (Fig. 1). Several gradient solutions were tested to achieve best separation of HCV virions from protein contaminants, while preserving their infectivity. Iodixanol gradients recovered >90% of the input infectivity in three fractions (Fig. S1E).

Compositional analysis of HCV virions by mass spectrometry. Transmission electron microscopy (TEM) of negatively stained purified virions, used as input material for proteomics analysis, revealed intact particles (Fig. 2A-B). Constituent proteins in HCV-enriched samples were resolved by SDS-PAGE and stained with Coomassie (Fig. 2C-D).

Viral proteins identified in purified HCV virions. As a first step, selected gel regions where Core, E1 and E2 are expected to migrate (~21, 35 and 70 kDa, respectively) were analyzed by liquid chromatography-mass spectrometry (LC-MS) to determine whether the purification protocols yielded sufficient material to detect the major HCV structural components. Both purification methods led to the identification of Core, E2 and the viral protease NS3 (Table 1). Table 1 lists the number of observed peptides and the percent sequence coverage of the protein (corrected for peptides unlikely to be observed by MS). The statistical score associated with the match, log (e), is also noted. Core displayed the highest relative abundance among the viral proteins using both purification methods, based on the number of unique and

total peptides and the sequence coverage achieved. Overall, the sample produced in SFM resulted in a lower LC-MS signal for viral proteins. This is in agreement with the electron microscopy images showing fewer virions in the input material (Fig. 2A). Digestion of virion-associated Core with trypsin resulted in the identification of peptides ending with arginine or lysine, as expected, with the exception of the most C-terminal peptide, which ended with phenylalanine (Fig. 3). To exclude that this was due to non-specific trypsin cleavage, the same sample was digested with Asp-N; with similar results (Fig. S2). The C terminus of the mature Core protein is produced by the host protease, SPP but the form present in mature virions has not been determined (5). Our results indicate that virion-incorporated Core is cleaved at phenylalanine 177. Since E2 is a heavily glycosylated protein, preliminary MS/LS sensitivity tests were conducted using a recombinant soluble E2 ectodomain (sE2; (6)). The identification of unique E2 peptides and total spectra were dose-dependent, with 6 unique peptides retrieved using the highest amount of purified protein (70 femtomoles) and a detection limit of ~ 4 femtomoles. Three of these peptides were also detected from mature virions, using either purification approach (Table 1 and Fig. S3). In the absence of PNGase F treatment, no peptides with N-linked glycans were identified, in agreement with previous studies (6). Given the lower amount of input material for the virus preparation in SFM, the gel slices of the Con1/Jc1 sample were cut in two and peptides were extracted with or without in-gel PNGase F digestion. Deglycosylation increased the sensitivity of detection for E2 from 3 to 4 unique peptides for the enzyme-treated slice, with the additional peptide containing an NXT glycosylation motif (Fig. S3G). While no E1 peptides were detected in PNGase F-treated virus preparations, E1 incorporation in virions could be inferred by the fact that the HCV-specific antibody used for the purification recognizes a conformational epitope encompassing E1/E2 (AR4A; (4)). Interestingly, the 70kDa gel region analyzed for E2 detection also contained peptides of the viral protease NS3. Three and one NS3 peptides were retrieved using both the tag- and antibody-mediated virus capture, respectively, suggesting that NS3 may be a virion component (Table 1).

Cellular proteins identified in purified HCV virions. Tag-mediated purification, although successful for isolating intact virions, resulted in high protein background with significant contamination from FBS-derived proteins, hampering the identification of host proteins that specifically associate to HCV. Therefore, we utilized the HCV neutralizing antibody AR4A as an alternative approach to purify HCV virions. As a negative control, the same amount of infectious particles was incubated with an HIV-specific antibody (B6). A protein was considered a candidate virion-associated factor if it satisfied all of the following criteria: a) is not a known exogenous contaminant such as keratin b) the log (e) score value does not exceed that of any protein identified from the decoy database of reversed protein sequences and c) both the main protein candidate identified by X!Tandem and its homologues had zero spectrum counts in the corresponding control sample. In total, 46 human proteins were specifically isolated with HCV virions (Table S2). These host factors were grouped into functional categories including RNA binding, regulation of gene expression, immunological and viral processes, intracellular transport, lipid metabolism and endocytosis (Fig. 4 and Table S3). Although apolipoproteins are known components of LVPs, they are not in the list of HCV-associated host factors according to the stringent inclusion criteria, because some peptides were also found in the control lane. Nevertheless, human apoE, apoB-100, apoA-II, apoC-II and C-III were enriched in purified HCV (Table S4).

Validation of virion-associated host proteins. To corroborate the proteomics data, 12 candidate cellular proteins were validated in follow-up studies by RNA interference (Table 2). These host

477
478
479
480
481
482
483
484
485
486
487
488
489
490
491
492
493
494
495
496
497
498
499
500
501
502
503
504
505
506
507
508
509
510
511
512
513
514
515
516
517
518
519
520
521
522
523
524
525
526
527
528
529
530
531
532
533
534
535
536
537
538
539
540
541
542
543
544

factors were prioritized based on the following criteria: a) number of observed peptides ≥ 3 ; b) $\log(e) \leq -7$ and c) previous implication in HCV or other viral infections, based on pubmed search. siRNA smart pools targeting the HCV genome and the entry receptor CD81 were used as positive controls for inhibition of viral infection in our functional assays (Fig. 5). ApoB-100 and ApoA-I siRNAs were also included in the analysis, as we previously demonstrated specific incorporation of these host-derived proteins in infectious HCV particles (3). Two days post-transfection with siRNAs, Huh-7.5 cells were challenged with Con1/Jc1 at low multiplicity of infection (MOI) and the number of NS5A positive cells and viral genomes released in the culture media was measured 72 hours later by FACS and RT-qPCR, respectively (Fig. 5). Therefore, this assay mainly looked at the impact of protein downregulation on secondary rounds of infection, determining a cumulative effect of the host factors on HCV propagation rather than discriminating between individual steps of the virus life cycle. Cell viability was measured by FACS from the same set of samples at the time of harvesting (Fig. S4B). mRNA expression levels of the targeted host factors were measured by real-time RT-PCR to confirm decreased expression of the intended gene by specific siRNAs (Fig. S4C). A striking decrease in the number of infected cells (Fig. 5A, C and S4) and extracellular viral genomes (Fig. 5B-C) was observed in cells silenced for the nucleoporin Nup98. This was paralleled by a 2-logs reduction in viral titers, when cell culture media derived from siRNA-transfected cells was inoculated onto naïve Huh-7 cells (Fig. 5D). Interestingly, silencing of SCYL2 and PTGFRN resulted in a 75 and 60% increase in HCV infection, respectively, suggesting an antiviral activity for these host factors. Finally, moderate inhibition of infection (~ 50%) was observed in cells where endogenous SLC3A2, TMEM109, ATP1A1 and SGTA were downregulated.

Nup98 interacts with Core and re-localizes to cytosolic lipid droplets (cLD) in infected cells. Given the profound inhibition of infection upon Nup98 silencing, we further investigated the role of this protein in HCV biology. Since Nup98 was found in HCV particles, we tested whether it bound to virion structural components. We showed that Core specifically co-immunoprecipitates with endogenous Nup98 (Fig. 6A). In physiological conditions, Nup98 localizes at the nuclear envelope, being a component of the nuclear pore complex (NPC) (7). Therefore, the role of Nup98 in HCV infection and its packaging into virions was unexpected considering that HCV replicates in the cytoplasm. To understand where the interaction between Nup98 and Core occurs, we performed immunofluorescence and electron microscopy (iEM) studies of infected Huh-7.5 cells. Differences in Nup98 subcellular distribution were observed at early versus late stages of infection. Initially, Nup98 staining is comparable to uninfected cells, mainly localizing at the nuclear envelope. In contrast, 6 days post-infection, Nup98 is enriched on large, round cytoplasmic structures where also Core localizes (Fig. S5A-B). Core is known to accumulate on cLD, cytoplasmic organelles for lipid storage, prior to being utilized for the nucleation of viral capsids (8). To confirm that Core and Nup98 were co-localizing on cLD, we used the Tokuyasu technique for immunolabelling of cryosections (9). The expected staining of Core on the surface of cLD was observed. Furthermore, Nup98 was shown to re-localize to cLD, while retaining its physiological localization at the nuclear envelope (Fig. 6B). Co-staining with Core and Nup98-specific antibodies by iEM confirmed that the two proteins co-localize on the surface of cLD in infected cells (Fig. 6B and S5C).

Nup98 is required for HCV morphogenesis. To dissect the role of Nup98 in HCV biology, Huh-7.5 cells were transfected with lentiviral particles encoding either irrelevant or Nup98-specific shRNAs (Fig. 7). The two cell lines were compared using viral assays that looked at specific steps of the HCV life cycle. HCV infection was impaired in cells where Nup98 protein

expression was downregulated, as shown by the reduction of intracellular Core levels (Fig. 7A). The negative impact of Nup98 silencing on infection was overcome in a dose-dependent manner by using higher MOI, suggesting that the block is not at the level of virus entry or early steps of infection (Fig. 7B). Accordingly, using a luciferase-reporter Jc1 virus, we showed that HCV replication and translation were comparable between shIRR and shNup98 cells (Fig. 7C). In contrast, the amount of both intracellular and extracellular infectious particles produced by shNup98 cells was reduced by 50% and 90%, respectively compared to control cells, indicating a role for Nup98 in the late steps of virion biogenesis (Fig. 7D).

Discussion

In the last decade, substantial progress in growing HCVcc has been made by using highly permissive cell lines and by selecting more fit viral genomes with adaptive mutations (10). Nevertheless, HCVcc titers remain in the range of 10^5 - 10^6 tissue culture infectious dose₅₀ (TCID₅₀) per ml, which is approximately 100 to a 1000-fold less than other enveloped viruses for which protein composition has been determined (1). If higher virus yields are achieved when serum is added to the culture media, contamination by highly abundant serum proteins compromises the ability to detect cellular proteins that are anticipated to be packaged into HCV virions in low copy numbers (Fig. 2). Furthermore, poor stability of virions makes the purification process extremely time-sensitive, limiting the number of purification steps that can be undertaken before most of the infectivity is lost (11). Finally, propensity to forming aggregates has been observed, preventing tandem affinity purification approaches (Fig. S1).

We undertook appropriate complementary approaches to compositional studies of extracellular HCV virions, using different viral genomes and affinity purification methods. Up to 15 liters of virus-containing supernatant were produced for this study and culture media was harvested frequently and stored at 4C to prevent virus inactivation (Fig. 1). More infectious virus particles (~ 5-10 folds) were being produced using FBS-containing media and these virions were better captured using tag- rather than antibody-mediated purification methods (3). Accordingly, a better sequence coverage of viral proteins was achieved by LC/MS using HCV samples produced in serum. Conversely, HCV isolation via glycoprotein-specific antibodies was more effective with preparations in SFM and resulted in significantly cleaner virion pull downs (Fig. 2). However, lower viral titers were achieved in SFM, hampering further fractionation approaches by ultracentrifugation.

Despite these differences, both approaches led to the identification of the same set of viral proteins, with Core displaying the highest sequence coverage (Table 1). Previous studies have shown that Core is cleaved by SPP at Phe 177 and that aa 1-177 of the protein are necessary and sufficient for HCV infectivity (5, 12). Using purified HCV virions fractionated over buoyant density gradient, we now determined that the C-terminus of Core packaged in infectious particles is Phe 177 (Fig. 3 and S2).

In addition to the expected structural viral proteins, the protease NS3 was also identified in virions produced in FBS as well as SFM, using different purification methods (Table 1). A possible explanation for this may be that incoming HCV particles would benefit from having a viral protease that can promptly inactivate cytoplasmic viral sensors upon capsid uncoating, prior to the formation of the membranous web. Alternatively, given its role in HCV assembly, NS3 may be incorporated in virions by proximity (2). The low signal compared to Core and E2 is consistent with the expectation of the protease not being incorporated in high-copy numbers.

The present study reveals an intimate interplay between HCV and the host in the make-up of infectious particles, with 46 po-

tential cellular proteins incorporated into mature virions (Table S2), belonging to a variety of functional classes (Fig. 4). While it is unclear whether all these cellular proteins represent true virion components or are only peripherally associated to HCV particles, some of them were previously linked to viral processes (Table S3) and are specifically regulated during HCV infection (13).

Two of these proteins, PTGFRN and SCYL2, display antiviral roles not only against HCV (Fig. 5 and S4) but also other pathogens. PTGFRN (also called CD9P-1 or EWI-F) inhibits the ability of hepatocytes to support Plasmodium sporozoite infection by interacting with CD81 (14). Interestingly, PTGFRN was shown to be upregulated in HCV-infected cells (13). The IFN-stimulated gene SCYL2 is a component of clathrin-coated vesicles, involved in membrane trafficking between the trans-Golgi and endosomes and it was shown to restrict HIV release by inhibiting the viral protein Vpu (15). Further investigations will be required to determine how these host factors counteract HCV infection and whether they can be considered bona fide restriction factors.

Conversely, Nup98 displayed the strongest pro-viral phenotype, with a profound reduction in viral genome release and infectious titers upon silencing (Fig. 5). A previous study identified Nup98 as an important host protein for HCV infection (16). Here, we show for the first time that Nup98 is co-purified with extracellular HCV virions (Table 2), physically interacts with Core (Fig. 6 and S5) and is specifically required for late stages of the HCV life cycle – assembly/maturation (Fig. 7). Follow up studies will determine whether Nup98's impact on HCV biogenesis is direct or can also be explained by Nup98 modulation of cellular gene expression.

Nup98 dynamically associates to the NPC, where it regulates nucleocytoplasmic transport of mRNAs and proteins (7). We propose that HCV hijacks Nup98 physiological functions to transport HCV structural components from different cellular compartments, thus coordinating virion morphogenesis. Accordingly, several HCV proteins, including Core, contain functional nuclear localization signals (NLS) and nuclear export signals (NES) sequences that are required to bind cargo proteins and cross the NPC (17). This would be in agreement with the model suggested by Neufeldt et al, which hypothesizes the insertion of NPC in the cytoplasm of infected cells to compartmentalize virus replication/assembly (16). To date, viruses have been described to target the NPC to cross the nuclear envelope and/or to control host transcription. In contrast, our proteomics, biochemical and ultrastructural data suggest a novel mechanism of Nup98 exploitation to aid virus assembly.

In summary, we report the first compositional analysis of extracellular HCV particles. Future studies will address the func-

tional roles that other HCV-associated host factors may fulfill during specific steps of the virus life cycle. This will further our understanding of the host contribution to HCV propagation and pathogenesis.

Materials and Methods

Virion Purification. HCV stocks were created by electroporating viral RNA into Huh-7.5.1 cells (18). Cells were switched to low-serum (1.5% FBS) or serum free (SFM) media 12 hours post electroporation (hpe) and virus-containing media was harvested every 3-6 hours up to 5 days post electroporation. Viral supernatants were concentrated in a stirred ultrafiltration cell (Model 8400 with 100-kDa MWCO membranes; Millipore) and purified over heparin column (GE Hitrap Heparin). Heparin-bound HCV was eluted with 0.02M Tris-HCl pH 7.4; 0.5M NaCl and dialyzed with PBS1X using Amicon-Ultra centrifugation devices (regenerated cellulose, low-protein binding capacity; Millipore, MWCO 100kDa). Heparin-eluted Con1/Jc1 was incubated with ProtA-coated magnetic beads (Bio-Adembeads; Ademtech) conjugated to antibodies specific to HCV (AR4A) or HIV (B6) envelope glycoproteins and eluted in SDS buffer. Heparin-eluted clone 2-His/OST (tag) and wild-type (wt) viruses were fractionated over a 10-40% (w/v) iodixanol buoyant density gradient (Optiprep; Sigma) (3). Fractions with the highest infectivity were incubated with His-Dynabeads (Invitrogen) for 1h at RT in the presence of 20mM imidazole and protease inhibitors. Bound particles were washed 50mM imidazole and eluted with 900mM imidazole (in PBS1X, pH 7.7).

Proteomics analysis. Gel lanes were sliced in 1 mm intervals and slices were pooled into 6 samples. Slices were cubed, destained with 50% v/v acetonitrile in 50 mM ammonium bicarbonate. To deglycosylate proteins, gel pieces were incubated with 80µl of PNGase F (11 units/µl; New England Biolabs) in 50 mM sodium phosphate pH 7.5 at 37°C overnight, then washed four times with water the next day. Proteins were digested overnight in 3.1ng/µl trypsin (Promega, Madison, WI) in 25 mM ammonium bicarbonate. Peptides were extracted with 2.5 mg/ml POROS R2 20 µm beads (Life Technologies, Grand Island, NY) in 5% formic acid, 0.2% TFA on a shaker at 4°C for 24 hours. Digests were desalted on Stage Tips, eluted, concentrated by SpeedVac, and loaded onto a 75 µm ID Picofrit column (New Objective, Woburn, MA) packed in-house with 6 cm of reverse-phase C18 material (5 µm particles, 300 Å pores, YMC-Gel ODS-A, YMC, Allentown, PA). Peptides were gradient-eluted (using 0.1 M acetic acid, and 0.1 M acetic acid in 70% acetonitrile, flow rate 200 nl/min) into an LTQ-Orbitrap-XL mass spectrometer (Thermo Fisher Scientific, Waltham, MA) acquiring data-dependent CID fragmentation spectra. Using the X!Tandem algorithm, raw data were searched against databases of human, bovine, and HCV protein sequences, as well as a decoy database of reversed protein sequences.

Detailed methods can be found in SI Materials and Methods.

ACKNOWLEDGMENTS. The authors are grateful to Dr. Joseph Marcotrigiano (Rutgers University) for providing sE2, Dr. Mansun Law (The Scripps Research Institute) for the AR4A and B6 antibodies, and Harishabh Khalsa for assistance with data analysis. The authors also thank Dr. Michael Rout (The Rockefeller University) and Dr. Beatriz Fontoura (UT Southwestern) for insightful discussions. This work was supported by National Institutes of Health Grants (to C.M.R.), The Greenberg Medical Research Institute and The Starr Foundation. M.L. was supported by Departmental start-up funds (King's College London), M.T.C. is the recipient of a Rockefeller University Women & Science Fellowship. Funding for MK was provided by Deutsche Forschungsgemeinschaft (DFG).

- Maxwell KL & Frappier L (2007) Viral proteomics. *Microbiology and molecular biology reviews* : *MMBR* 71(2):398-411.
- Lindenbach BD & Rice CM (2013) The ins and outs of hepatitis C virus entry and assembly. *Nat Rev Microbiol* 11(10):688-700.
- Catanese MT, et al. (2013) Ultrastructural analysis of hepatitis C virus particles. *Proceedings of the National Academy of Sciences of the United States of America* 110(23):9505-9510.
- Giang E, et al. (2012) Human broadly neutralizing antibodies to the envelope glycoprotein complex of hepatitis C virus. *Proc Natl Acad Sci U S A* 109(16):6205-6210.
- Okamoto K, et al. (2008) Intramembrane processing by signal peptide peptidase regulates the membrane localization of hepatitis C virus core protein and viral propagation. *Journal of virology* 82(17):8349-8361.
- Whidby J, et al. (2009) Blocking hepatitis C virus infection with recombinant form of envelope protein 2 ectodomain. *Journal of virology* 83(21):11078-11089.
- Griffis ER, Xu S, & Powers MA (2003) Nup98 localizes to both nuclear and cytoplasmic sides of the nuclear pore and binds to two distinct nucleoporin subcomplexes. *Molecular biology of the cell* 14(2):600-610.
- Miyanari Y, et al. (2007) The lipid droplet is an important organelle for hepatitis C virus production. *Nature cell biology* 9(9):1089-1097.
- Tokuyasu KT (1973) A technique for ultracytometry of cell suspensions and tissues. *The Journal of cell biology* 57(2):551-565.
- Catanese MT & Dörner M (2015) Advances in experimental systems to study hepatitis C virus in vitro and in vivo. *Virology* 479-480:221-233.
- Ciesek S, et al. (2010) How stable is the hepatitis C virus (HCV)? Environmental stability of HCV and its susceptibility to chemical biocides. *J Infect Dis* 201(12):1859-1866.
- Kopp M, Murray CL, Jones CT, & Rice CM (2010) Genetic analysis of the carboxy-terminal region of the hepatitis C virus core protein. *Journal of virology* 84(4):1666-1673.
- Diamond DL, et al. (2010) Temporal proteome and lipidome profiles reveal hepatitis C virus-associated reprogramming of hepatocellular metabolism and bioenergetics. *PLoS Pathog* 6(1):e1000719.
- Charrin S, et al. (2009) The Ig domain protein CD9P-1 down-regulates CD81 ability to support Plasmodium yoelii infection. *J Biol Chem* 284(46):31572-31578.
- Miyakawa K, et al. (2012) Interferon-induced SCYL2 limits release of HIV-1 by triggering PP2A-mediated dephosphorylation of the viral protein Vpu. *Science signaling* 5(245):ra73.
- Neufeldt CJ, et al. (2013) Hepatitis C virus-induced cytoplasmic organelles use the nuclear transport machinery to establish an environment conducive to virus replication. *PLoS pathogens* 9(10):e1003744.
- Levin A, et al. (2014) Functional characterization of nuclear localization and export signals in hepatitis C virus proteins and their role in the membranous web. *PLoS one* 9(12):e114629.
- Lindenbach BD, et al. (2005) Complete replication of hepatitis C virus in cell culture. *Science* 309(5734):623-626.
- Jones CT, et al. (2010) Real-time imaging of hepatitis C virus infection using a fluorescent cell-based reporter system. *Nat Biotechnol* 28(2):167-171.
- Andrus L, et al. (2011) Expression of paramyxovirus V proteins promotes replication and spread of hepatitis C virus in cultures of primary human fetal liver cells. *Hepatology* 54(6):1901-1912.
- Catanese MT, et al. (2013) Different requirements for scavenger receptor class B type I in hepatitis C virus cell-free versus cell-to-cell transmission. *Journal of virology* 87(15):8282-8293.